

TRACE: Time SeRies PArameter EffiCient FinE-tuning

Yuze Li^{1a}, Wei Zhu^b

^a*Shenzhen International Graduate School, Tsinghua University, Shenzhen, China*

^b*School of Science, University of Hong Kong, Hong Kong, China*

Abstract

We propose an efficient fine-tuning method for time series foundation models, termed TRACE: Time Series Parameter Efficient Fine-tuning. While pre-trained time series foundation models are gaining popularity, they face the following challenges: (1) Time series data exhibit significant heterogeneity in frequency, channel count, and sequence lengths, necessitating tailored fine-tuning strategies, especially for long-term forecasting. (2) Existing parameter-efficient fine-tuning (PEFT) methods, such as LoRA, are not directly optimized for the unique characteristics of time series data.

To address these challenges, our TRACE framework introduces two key innovations: (1) Gated DSIC (Gated Dynamic Simulation Importance Calculation), a less biased LoRA module selection mechanism that ensures conditional parameter consistency before and after masking; and (2) Reconstructed forecasting heads for long-term forecasting tasks, which achieve comparable or superior performance to linear probing while drastically reducing parameter counts.

Extensive experiments on long-/short-term forecasting, anomaly detection and natural language tasks across diverse datasets, coupled with ablation studies, validate the effectiveness of our method.

Keywords: fine-tuning, time series, foundation model, forecasting

¹Corresponding Author. Email: liyuze23@mails.tsinghua.edu.cn

1. Introduction

Pre-trained time series foundation models (e.g., MOMENT [1]) have demonstrated strong generalization across diverse forecasting and anomaly detection tasks. However, their effective adaptation to downstream applications remains hindered by two key challenges in fine-tuning.

First, standard full fine-tuning is computationally expensive and often infeasible on resource-constrained hardware. In contrast, linear probing—freezing the backbone and tuning only the forecasting head—is efficient but suboptimal: it fails to exploit the rich temporal representations encoded in intermediate layers. This limitation is especially severe in **long-horizon forecasting**, where the forecasting head itself can contain millions of parameters (e.g., $> 35M$ for a 720-step horizon in MOMENT), leading to overfitting and degraded performance.

Second, existing parameter-efficient fine-tuning (PEFT) methods like LoRA were designed for natural language tasks and do not account for the unique structure of time series data. Naive application of such methods suffers from **biased importance estimation** during module selection, resulting in sub-optimal adaptation.

To address these issues, we propose **TRACE** (Time Series Parameter Efficient Fine-tuning), a novel framework with two core components:

- (1) **Reconstructed forecasting heads** that factorize the original forecasting layer, reducing its parameter count by over 70% while improving or matching performance.
- (2) **Gated DSIC (Gated Dynamic Simulation Importance Calculation)**, a debiased LoRA module selection mechanism that simulates post-pruning contexts via Monte Carlo masking to accurately estimate module importance.

Our contributions are summarized as follows:

- (1) We design lightweight, high-performance forecasting heads tailored for long-horizon time series tasks.
- (2) We introduce Gated DSIC, a novel PEFT strategy that mitigates evaluation bias and enables dynamic, reversible LoRA pruning.
- (3) We conduct extensive experiments across long/short-term forecasting, anomaly detection, and even NLP benchmarks, showing that TRACE consistently outperforms full fine-tuning, linear probing, and prior PEFT baselines.

(4) We demonstrate that our method generalizes beyond time series, achieving state-of-the-art results on GLUE and QA tasks with minimal trainable parameters.

2. Related work

2.1. Time Series Modeling

Development of Time Series Forecasting: Time series forecasting has progressed from statistical methods to machine learning, deep learning, Transformer-based architectures, and time series foundation models.

Statistical Methods: Early methods like Moving Average (MA) and Exponential Smoothing [2] smooth trends but fail to capture complex dynamics. ARIMA [3] improves accuracy by integrating Autoregressive (AR) and MA components but struggles with nonlinear relationships. VAR [4] models multivariate relationships but suffers from dimensionality issues. These methods are limited to univariate modeling and cannot effectively use covariates.

Machine Learning Methods: Gradient boosting trees (e.g., XGBoost [5], LightGBM [6]) leverage feature engineering strategies, such as lag features and sliding window statistics, to model nonlinear patterns. While outperforming statistical methods, their performance depends heavily on feature quality and fixed window lengths limit long-term dependency modeling.

Deep Learning Methods: RNNs and variants like LSTM [7] and GRU [8] capture temporal dependencies but suffer from inefficiency and vanishing gradients for long-range dependencies. TCNs [9] expand receptive fields via dilated convolutions but are constrained by fixed kernels.

Transformer Architectures: Transformers [10] excel in capturing global dependencies and enabling parallel computation. Innovations include sparse attention (Informer [11]), channel independence modeling (iTransformer [12]), frequency-domain enhancement (FEDformer [13]), and causality constraints (PathTST [14]). Challenges remain, including quadratic complexity with sequence length and limited explicit modeling of inherent time series attributes.

Time Series Foundation Models: Recent foundation models leverage large-scale pretraining on heterogeneous data to learn general representations. Key innovations include multimodal fusion, prompt learning, and support for zero-shot or few-shot forecasting. These models break feature engineering limitations, enhance cross-domain generalization, and handle multivariate/multimodal inputs. Current research focuses on efficient pretraining, interpretability, and lightweight designs.

2.2. Time Series Foundation Models

Time Series Foundation Models follow two main approaches: (1) pre-training from scratch on time series data, and (2) adapting large language models (LLMs) for time series tasks.

Approach 1: Pre-training from Scratch. This approach trains models directly on large-scale time series data (e.g., sensor, financial, or weather data) to capture long-term dependencies, periodicity, and trends using self-supervised tasks like forecasting, imputation, or generation. These models are powerful for time-series tasks but require massive labeled data and high computational costs. Notable examples include TimeGPT [15], a Transformer-based model supporting zero-shot transfer; Tempo [16], a diffusion-based generative model for multivariate time series; TimesFM [17], a decoder-only architecture with hierarchical time aggregation for irregular data; and Moirai [18], a unified model with multi-task pretraining for long sequences.

Approach 2: Adapting LLMs for Time Series. This approach maps time series data into textual or other modalities using cross-modal alignment, leveraging LLMs' semantic understanding for tasks like trend description or multimodal reasoning. Challenges include bridging the gap between continuous time series and discrete text, as well as handling causality conflicts with LLM position encodings. Key works include LLMTIME [19], which discretizes time series into "time tokens" for forecasting via text generation; TEST [20], which converts time series into natural language templates for zero-shot forecasting; TimeLLM [21], aligning time series with LLMs using embeddings; TEMPO [16], jointly encoding time series and text for domain-specific tasks; and Lag-Llama [22], fine-tuning Llama with lag operators for univariate forecasting.

3. Preliminaries

Transformer-based Models. Transformer [10] consists of L stacked blocks, each with multi-head attention (MHA) and feed-forward network (FFN) modules. For input $X \in \mathbb{R}^{n \times d}$, MHA computes:

$$\text{MHA}(X) = \text{Concat}(\text{head}_1, \dots, \text{head}_h)W_o, \quad (1)$$

$$\text{head}_i = \text{Softmax}(XW_{q_i}(XW_{k_i})^\top / \sqrt{d_h})XW_{v_i}, \quad (2)$$

where $W_o \in \mathbb{R}^{d \times d}$, $W_{q_i}, W_{k_i}, W_{v_i} \in \mathbb{R}^{d \times d_h}$, and $d_h = d/h$. The FFN uses two linear layers:

$$\text{FFN}(X) = \text{ReLU}(XW_{f_1} + b_1)W_{f_2} + b_2. \quad (3)$$

Residual connections and layer normalization follow both sub-modules. ReLU is often replaced by Gated Linear Units (GLU) [23]:

$$\text{GLU}(X) = (XW_{f_0} + b_0) \otimes \sigma(XW_{f_1} + b_1), \quad (4)$$

where \otimes is element-wise multiplication and σ is the sigmoid function.

Patching. Time series forecasting benefits from treating subsequences (patches) as tokens rather than individual time points. This approach captures local semantic information and enhances predictive representations [14].

Channel Independence. Multivariate time series can be modeled with channel independence, where each token represents data from a single channel [14]. This simplifies the model and allows learning channel-specific dynamics.

MOMENT Model. MOMENT [1] is a Transformer-based time series foundation model pretrained on diverse data using masked prediction. It supports long-term/short-term prediction, anomaly detection, and classification. MOMENT-base consists of 12 Transformer encoders with $d = 768$, $h = 12$, and $d_m = 3072$. Its FFN uses GLU:

$$\text{FFN}(X) = (XW_{f_0} \otimes \text{GELU}(XW_{f_1}))W_{f_2}. \quad (5)$$

Input time series ($T = 512$) are divided into $N = 64$ non-overlapping patches ($P = 8$). MOMENT leverages pre-training to capture complex temporal dependencies. We use MOMENT-base to validate TRACE’s effectiveness unless otherwise specified.

4. Our method

4.1. Gated DSIC: Mitigating Bias in LoRA Module

Parameter-efficient fine-tuning (PEFT) methods like LoRA offer a promising alternative to full fine-tuning. However, naively applying them to time series foundation models is suboptimal. For instance, AdaLoRA parameterizes the weight update via singular value decomposition (SVD) and prunes low-importance singular values to adapt the rank dynamically. While effective in some domains, AdaLoRA faces notable challenges in time-series scenarios. Its SVD-based pruning prioritizes singular values reflecting global feature importance, potentially overlooking critical local signals such as abrupt anomalies or short-term seasonality. Furthermore, its static, irreversible pruning risks underfitting if early-stage pruning discards modules that become relevant later in training.

To address these limitations, we propose Gated Dynamic Simulation Importance Calculation (Gated DSIC), a less biased LoRA module selection mechanism. Gated DSIC introduces a learnable gate for each LoRA module, enabling dynamic and reversible masking. Crucially, it employs a Monte Carlo simulation during the importance evaluation phase to ensure that the importance score of a module is calculated under conditions that mimic the post-masking state, thereby mitigating the bias inherent in sequential, deterministic pruning strategies like AdaLoRA. This ensures conditional parameter consistency before and after masking, allowing the model to recover suppressed modules if needed (e.g., when seasonal patterns re-emerge). Concretely, each LoRA module is associated with a gate whose activation is determined by a less biased importance score estimated via repeated random masking on the validation set. The detailed algorithm is presented in Section 4.3.

Figure 1 illustrates the comparison between the TRACE method and the full LoRA fine-tuning model architecture.

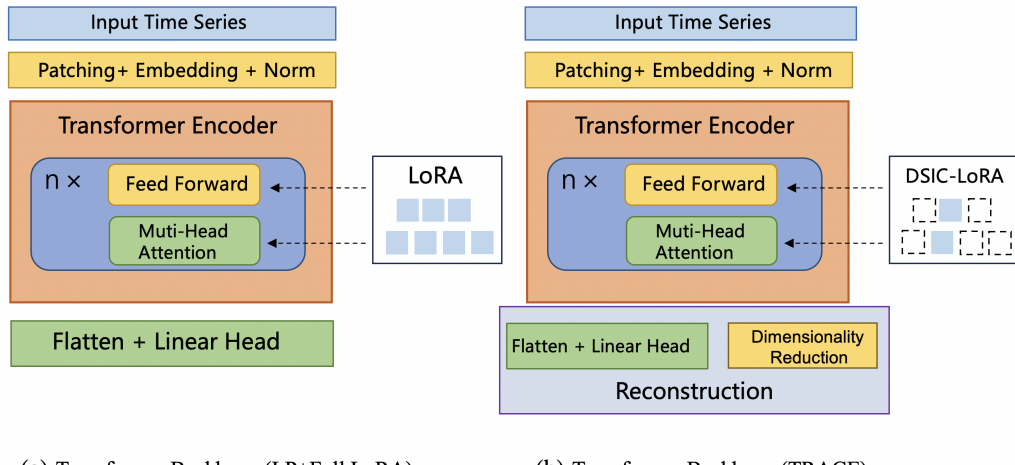


Figure 1: architecture of our method:(a) Represents the default model architecture, which consists of multiple stacked Transformer encoders. LoRA modules are added to all linear layers at each level, and the forecasting head is a linear predictor. Fine-tuning is performed using linear probing and full LoRA adaptation.(b) Represents the TRACE method: LoRA integration follows the Gated DSIC approach, and for long-term forecasting tasks, the forecasting head is dimensionally reduced and reconstructed.

Table 1: Comparison of forecasting head parameters across different horizons and reduction under varying β values

Horizon	β	Head Parameters	Reduced	Reduction Percentage
192	4	9,437,184	2,506,752	73.4%
	8	9,437,184	1,253,376	86.7%
	16	9,437,184	626,688	93.4%
720	4	35,389,440	8,994,816	74.6%
	8	35,389,440	4,497,408	87.3%
	16	35,389,440	626,688	98.2%

4.2. Reconstruction of Long-horizon Forecasting

The standard linear forecasting head in models like MOMENT, parameterized by a matrix $\mathbf{W} \in \mathbb{R}^{(N \times d) \times H}$, becomes prohibitively large for long-horizon forecasting (e.g., $H = 720$), often exceeding 35M parameters. While small relative to the full backbone, this introduces significant overfitting risk and computational burden during fine-tuning.

To address this, we propose reconstructing the forecasting head via low-rank factorization, reducing its parameter count while preserving or enhancing predictive performance. As illustrated in Figure 2, our approach decomposes the original weight matrix \mathbf{W} into two smaller matrices:

$$\mathbf{W}_{\text{recon}} = \mathbf{W}_1 \cdot \mathbf{W}_2, \quad \text{where} \quad \mathbf{W}_1 \in \mathbb{R}^{(N \times d) \times d'}, \quad \mathbf{W}_2 \in \mathbb{R}^{d' \times H}, \quad (6)$$

and $d' = d/\beta$ is the reduced embedding dimension, controlled by the reduction factor β .

This reconstruction reduces the parameter count from $\mathcal{O}(NdH)$ to $\mathcal{O}(Nd^2/\beta + dH/\beta)$, achieving reductions of up to 98.2% (see Table 1) with minimal performance loss. We experiment with four variants—Projection Down (Proj-Down), Feature Truncation (LessFeature), Average Pooling (AvgPool), and 2D Convolution (Conv2D)—each offering different trade-offs between efficiency and representational capacity.

Our experiments (Section 5.5.2) show that ProjDown and AvgPool consistently outperform the baseline linear probing, validating the effectiveness of our reconstruction strategy.

Appendix A is a concise description of the reconstruction operations applied to the forecasting head. The parameter d represents the embedding dimension for each patch (subsequence), with $d = 768$ in MOMENT. To

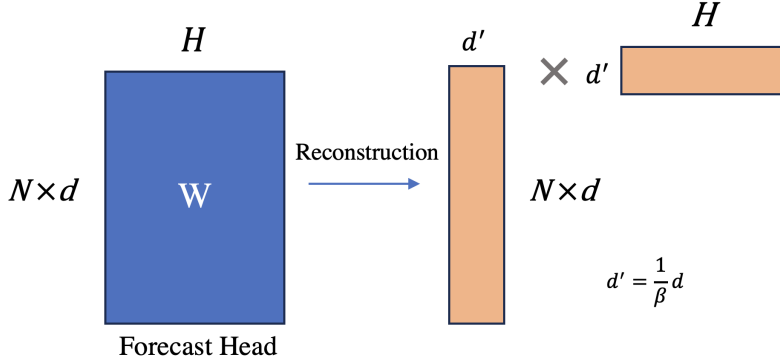


Figure 2: Illustration of forecasting head reconstruction. The original large matrix $\mathbf{W} \in \mathbb{R}^{(N \times d) \times H}$ is factorized into two smaller matrices, reducing the embedding dimension from d to $d' = d/\beta$. This significantly cuts the number of trainable parameters without sacrificing predictive power.

leverage the pre-trained model’s predictive capabilities and reduce overfitting, we reduce d since patch length limits information content.

4.3. Our Gated DSIC method

4.3.1. Learnable Gating for Dynamic LoRA Control

We propose a method to identify the most important and effective LoRA modules, allowing for efficient fine-tuning within a limited parameter budget.

To enable dynamic and reversible selection of LoRA modules during parameter-efficient fine-tuning, we introduce a **learnable scalar gate** $g_{ij} \in \mathbb{R}$ for the j -th LoRA module in the i -th Transformer layer. This gate multiplicatively modulates the low-rank update, yielding the adapted layer output:

$$h_{ij} = W_{ij}^{(0)}x + g_{ij} \cdot \Delta x_{ij} = W_{ij}^{(0)}x + g_{ij} \cdot B A x,$$

where $W_{ij}^{(0)}$ denotes the pre-trained weight matrix, and $A \in \mathbb{R}^{r \times d_2}$, $B \in \mathbb{R}^{d_1 \times r}$ are the low-rank adaptation matrices with rank $r \ll \min(d_1, d_2)$. The gate g_{ij} is initialized to 1 and optimized jointly with A and B via backpropagation.

Crucially, the importance of each LoRA module is estimated through the magnitude of the gradient of the validation loss with respect to its gate:

$$I(g_{ij}) = \|\nabla_{g_{ij}} \mathcal{L}_{val}\| \tag{7}$$

This gradient reflects how sensitive the model’s performance is to perturbations in g_{ij} , providing a natural proxy for module contribution.

Taking MOMENT-base as an example, which consists of 12 Transformer encoder layers with 7 linear sub-layers each (Query, Key, Value, Output, and three FFN projections), this yields a total of 84 gates, denoted as $\mathcal{G} = \{g_{ij} \mid i = 1, \dots, 12; j = 1, \dots, 7\}$.

Once we have $I(g_{ij})$, we can prune the parameters of those LoRA modules that contribute less to the fine-tuning task. This helps reduce the parameter count and prevent overfitting.

Following common practice, we define the importance score of unmasked gates as the expected sum of gradient magnitudes:

$$I(g_{ij}) = \mathbb{E}_{(X,Y) \sim \mathcal{D}_{\text{val}}} \left[\sum_{t=1}^T \left| \frac{\partial \mathcal{L}_{\text{val}}}{\partial g_{ij}} \right| \right] \quad (8)$$

However, this method has a bias in evaluating importance. For example, when calculating the importance $I(g_{kl})$, the implicit assumption is that the effect of a small fluctuation Δg_{kl} on the overall loss is measured while keeping $|g_{ij}| = 1$ for all other $i \neq k$ and $j \neq l$. However, when we mask some of the LoRA Gates based on their importance rankings, the premise of this assumption changes, leading to bias in the importance evaluation. Specifically, for g_{kl} , assuming it remained unmasked and some other LoRA Gates were masked in one operation, we observe:

$$I(g_{kl} \mid g_{ij} = 1, g_{ij} \in \mathcal{G}) \neq I(g_{kl} \mid g_{mn} = 0, g_{mn} \in \tilde{\mathcal{G}} \text{ and } g_{pq} = 1, g_{pq} \notin \tilde{\mathcal{G}}) \quad (9)$$

where $\tilde{\mathcal{G}}$ denotes the set of masked LoRA Gates. Equation (9) demonstrates that the masking of some LoRA Gates will change the importance of the remaining unmasked LoRA Gates, thus introducing bias.

4.3.2. Our solution: Gated Dynamic Simulation Importance Calculation

As discussed in Section 4.3.1, the standard gradient-based importance evaluation (e.g., as used in AdaLoRA) is biased. This bias arises because the importance score for a LoRA module is calculated under the assumption that all other modules are active. However, during pruning, many other modules are masked (set to zero), which fundamentally alters the model’s context and thus the true contribution of the remaining modules. This inconsistency between the evaluation condition (all modules active) and the deployment condition (many modules masked) leads to an inaccurate and biased importance estimate.

To address this, we propose the Gated Dynamic Simulation Importance Calculation (Gated DSIC) method, which aims to reduce this evaluation bias by simulating the post-pruning context during the importance calculation phase. The core idea is to evaluate a module’s importance not in isolation, but within a dynamically changing coalition of other active and masked modules, thereby better approximating its true contribution in the final pruned model.

Specifically, our method performs a Monte Carlo simulation on the validation set. In each simulation trial, we randomly mask a subset of the LoRA gates. The importance of the remaining unmasked gates is then computed based on their gradients in this specific masked context. By repeating this process many times (M times) and averaging the importance scores across all trials, we obtain a more robust and less biased estimate of each module’s contribution. This procedure ensures that the importance evaluation condition is consistent with the diverse contexts the module will experience after pruning, leading to a more reliable selection of modules to retain.

The superiority of our approach in reducing bias is empirically validated by comparing its importance scores against the gold-standard Shapley Value method, as proposed in [24]. Following the protocol in [24], we compute the Shapley Values for each LoRA module in a MOMENT-base model fine-tuned on the ETTh1 dataset. We then compare the correlation between these Shapley Values and the importance scores generated by our Gated DSIC method and the gradient-based method used in AdaLoRA. As shown in Table 2, our method achieves a 63.3% correlation with the Shapley Values, while AdaLoRA’s method shows a significantly lower correlation of -22.1%. This strong alignment with the theoretically sound Shapley Value method demonstrates that Gated DSIC provides a much less biased estimation of module importance compared to conventional gradient-based approaches. This allows our method to achieve performance close to the Shapley-based selection while being computationally feasible (0.25 GPU hours vs. 27 GPU hours for Shapley computation).

To further illustrate this point, we visualize the LoRA module importance scores calculated by the three methods on a MOMENT-base model fine-tuned on ETTh1. As shown in Figure 3, the importance distribution generated by AdaLoRA (left) is highly concentrated, indicating a potential bias towards a small subset of modules. In contrast, the distribution from our Gated DSIC method (middle) exhibits a more diverse and balanced pattern, closely resembling the distribution produced by the Shapley Value method (right),

Table 2: Correlation of Importance Scores with Shapley Values. We compute the Spearman correlation between the importance scores from different methods and the ground-truth Shapley Values for LoRA modules in a MOMENT-base model fine-tuned on ETTh1.

METHOD	CORRELATION WITH SHAPLEY VALUE
Gated DSIC (Ours)	63.3%
AdaLoRA (Gradient-based)	-22.1%

which is considered the gold standard for credit assignment. This visual evidence corroborates our quantitative findings, confirming that Gated DSIC effectively mitigates the evaluation bias inherent in standard gradient-based pruning.

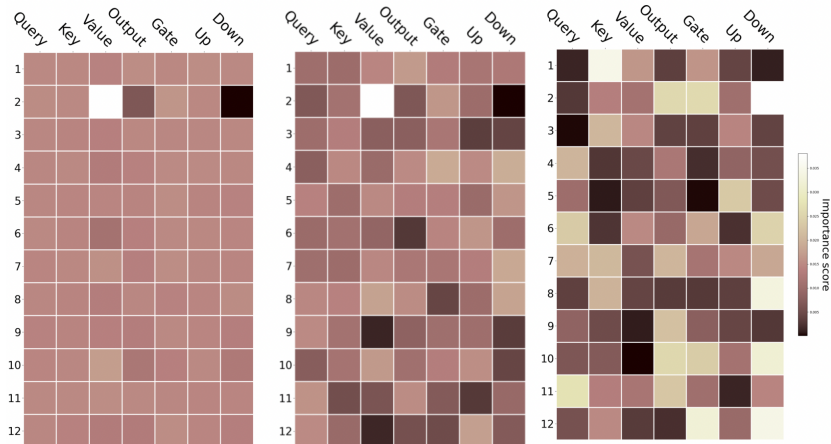


Figure 3: Visualization of LoRA Module Importance Scores. Left: AdaLoRA (Gradient-based). Middle: Gated DSIC (Ours). Right: Shapley Value. The color intensity represents the magnitude of the importance score, with darker shades indicating higher importance. The x-axis represents different LoRA module types (Query, Key, Value, Output, Gate, Up, Down), and the y-axis represents the Transformer layer number (1-12).

These quantitative and qualitative analyses confirm that Gated DSIC effectively mitigates the evaluation bias inherent in standard gradient-based methods. The detailed procedure of our method is as follows:

Stage 1: Joint Training

We simultaneously optimize the low-rank matrices $\{A, B\}$, reconstruction forecasting head H and the gating parameters $\mathcal{G} = \{g_{ij}\}$ on the training set.

The loss function is:

$$\mathcal{L}_{\text{train}} = \mathcal{L}_{\text{task}}(f(X; W_0 + g \cdot BA, H), Y) \quad (10)$$

Stage 2: Less Biased Importance Evaluation

We perform a Monte Carlo masking experiment on the validation set:

1. **Random Masking:** With probability p , randomly set some of the gates to 0, i.e., $g_{ij} \leftarrow 0$, and denote the masked set as $\tilde{\mathcal{G}} \subseteq \mathcal{G}$. The remaining gates are kept as 1. This operation is counted as k .
2. **Importance Calculation:** We compute the importance of the gates on the validation set \mathcal{D}_{val} :

$$I^{(k)}(g_{ij}) = \begin{cases} \mathbb{E}_{(X,Y) \sim \mathcal{D}_{\text{val}}} \left[\sum_{t=1}^T \left| \frac{\partial \mathcal{L}_{\text{val}}}{\partial g_{ij}} \right| \right] & \text{if } g_{ij} \notin \tilde{\mathcal{G}} \\ 0 & \text{if } g_{ij} \in \tilde{\mathcal{G}} \end{cases} \quad (11)$$

3. **Repeated Sampling:** Repeat the random masking operation M times, each time obtaining a different masked set $\tilde{\mathcal{G}}$ and corresponding importance scores $I^{(k)}(g_{ij})$.
4. **Average Gradient:** Take the average gradient importance across the M samples to obtain a less biased and stable evaluation:

$$\bar{I}(g_{ij}) = \frac{1}{M} \sum_{k=1}^M I^{(k)}(g_{ij}) \quad (12)$$

Figure 4 visualizes how our method calculates the importance score for each LoRA gate. In each of M independent trials, a random subset of LoRA gates is masked (indicated by grey boxes with 'x'). The gradient magnitude of the unmasked gates is then computed on the validation set. The final importance score for each gate (e.g., 0.31, 0.53) is obtained by averaging its gradient magnitudes across all M trials, as defined in Equation 12. This Monte Carlo simulation ensures that the evaluation context approximates the post-pruning state.

Gate Pruning

Based on $\bar{I}(g_{ij})$, we rank the gates and prune the $p\%$ gates with the lowest importance (set them to 0), thereby retaining the most effective LoRA modules. This process is repeated iteratively over training epochs.

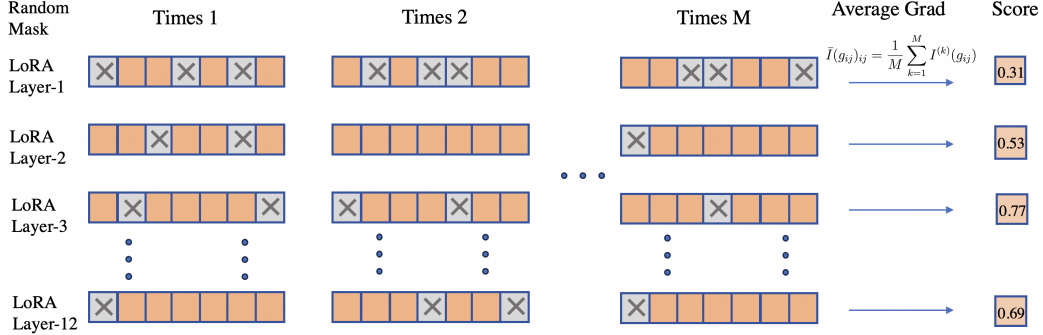


Figure 4: Illustration of the Gated DSIC Importance Scoring Process

Figure 5 depicts the iterative pruning process over T epochs. At each epoch t , we prune an additional $p\%$ of the currently unmasked LoRA gates based on their importance scores from Figure 4. This continues until the total number of pruned gates reaches the predefined budget (e.g., $T \times p\%$), achieving efficient fine-tuning with minimal parameter usage.

This method, through multiple random experiments, constructs model contexts that approximate the post-pruning state, leading to a more reliable and less biased importance estimation for LoRA gates.

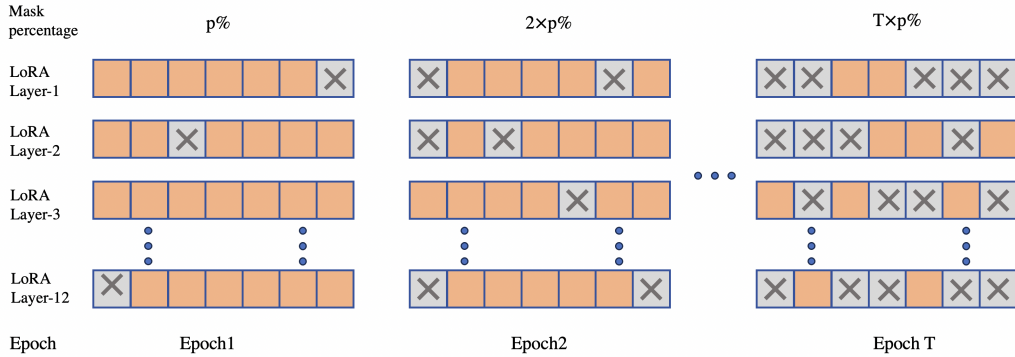


Figure 5: Illustration of the Iterative Pruning Schedule

4.3.3. Workflow

We present the complete calculation workflow for our Gated DSIC method:

Algorithm 1 The whole workflow of our Gated DSIC method

Input: Train dataset \mathcal{D}_{train} , Validation dataset \mathcal{D}_{val} ; total iterations T ; budget schedule $\{b^{(t)}\}_{t=0}^T$; hyperparameters p

```
1: for  $t=1, \dots, T$  do
2:   First, train for  $\alpha$  steps on the training dataset  $\mathcal{D}_{train}$ 
3:   for  $k=1, \dots, M$  do
4:     Random Masking: Randomly set  $p\%$  of the currently unmasked
       LoRA gates to 0, denoted as  $\tilde{\mathcal{G}}$ 
5:     Sample a batch from  $\mathcal{D}_{val}$  and compute the gradient  $\nabla \mathcal{L}(g, \mathcal{A}, \mathcal{B})$ 
6:     Compute the sensitivity  $I^{(k)}(g_{ij})$  for the LoRA gates  $g_{ij} \in \mathcal{G}/\tilde{\mathcal{G}}$ 
7:   end for
8:   Compute the average sensitivity for all LoRA gates:  $\bar{I}(g_{ij}) = \frac{1}{M} \sum_{k=1}^M I^{(k)}(g_{ij})$  and mask the top  $p\%$  ranked gates
9:   Continue training for  $\alpha$  steps, then repeat the process of masking the
      top  $p\%$  of LoRA gates until the parameter budget  $b$  is reached
10: end for
```

Output: $\tilde{\mathcal{G}}$

Algorithm 1 describes the Gated DSIC method. The procedure begins by dividing the data into a training set \mathcal{D}_{train} and a validation set \mathcal{D}_{val} . After training for α steps on the training set, we proceed with the following steps on the validation set: first, we randomly mask $p\%$ of the LoRA gates, then compute the sensitivity for the unmasked LoRA gates using equation(11). After repeating the experiment M times, we calculate the average sensitivity for each LoRA gate and mask the top $p\%$ gates. This process is repeated until the number of masked LoRA modules reaches the predefined parameter budget b . Finally, the method outputs the set of LoRA gates to be masked, $\tilde{\mathcal{G}}$.

We have evaluated the Gated DSIC method on these tasks: long-term time series forecasting, short-term forecasting, anomaly detection and natural language processing.

5. EXPERIMENTS

5.1. Datasets and Evaluation Metrics

Datasets. For forecasting and anomaly detection, we used subsets of the MOMENT dataset. Long-term forecasting tasks include ETTh1, ETTh2,

Table 3: Dataset Splits, Number of Channels, and Prediction Lengths for Different Tasks and Datasets

Task	Dataset	Channels	Series Length	Data Size (Train, Val, Test)
Long horizon forecasting (Informer)	ETTh1,ETTh2	7	{192,720}	(8033, 2785, 2785)
	ETTm1,ETTm2	7		(33953, 11425, 11425)
	Weather	21		(36280, 5175, 10444)
	Exchange	8		(4704, 665, 1422)
Short horizon forecasting (Monash)	M4-Yearly	1	6	(16099, 2301, 4600)
	M4-Quarterly	1	8	(16800, 2400, 4800)
	M4-Monthly	1	18	(33600, 4800, 9600)
	M3-Yearly	1	6	(451, 65, 129)
	M3-Quarterly	1	8	(529, 76, 151)
	M3-Monthly	1	18	(999, 144, 285)
Anomaly detection (TSB-UAD)	MITDB	1	-	(50%, -, 50%)
	ECG	1		
	MGAB	1		
	SVDB	1		

ETTm1, ETTm2 [25], Weather, and Exchange [11]. Short-term forecasting uses M4 and M3 from the Monash archive [26], consisting of Yearly (macroeconomic indicators, 5–50 years, horizon=6), Quarterly (sales/economic data, 10–100 quarters, horizon=8), and Monthly (retail/energy/weather data, 50–1000 months, horizon=18). Anomaly detection uses the TSB-UAD benchmark [27], with 1980 univariate time series annotated from 18 public datasets. We selected 9 series from MITDB, ECG, MGAB, and SVDB for experiments.

Metrics. We used multiple metrics commonly employed in task-specific benchmarks to evaluate each experiment, including MSE and MAE for long-term forecasting, and sMAPE for short-term forecasting. The vanilla F1 score is not suitable for time series tasks, as it ignores their sequential nature. Therefore, for anomaly detection performance, we use the widely accepted adjusted best F1 score.

5.2. Compared models

All of our models are based on the MOMENT-base pre-trained model. For the forecasting task, we compare the performance of MOMENT under four different modes: linear probing, full LoRA fine-tuning, reconstructed forecasting head, and TRACE fine-tuning. The details of these methods are as follows:

Forecasting: (1) *Linear Probing*: The model is linear-probed (MOMENT_{LP}) by freezing all parameters except for those in the reconstruction or forecast-

ing head. **(2) LoRA Fine-tuning:** Based on linear probing, LoRA modules are added to all linear layers for fine-tuning. **(3) Reconstructed Forecasting Head:** The forecasting head is reconstructed using the four methods in sec 4.2: *Proj Down*, *Avg Pool*, *Less Feature* and *Conv 2D*. **(4) AdaLoRA:** *ProjDown* forecasting head with AdaLoRA method. **(5) TRACE:** In addition to the reconstructed forecasting head, the Gated DSIC method is incorporated. The main model for TRACE uses the *Proj Down* method for dimensionality reduction in the forecasting head.

Anomaly Detection: **(1) Linear Probing:** The model is linear-probed (MOMENT_{LP}) by freezing all parameters except for those in the reconstruction or forecasting head. **(2) LoRA Fine-tuning:** Based on linear probing, LoRA modules are added to all linear layers for fine-tuning. **(3) TRACE:** The DSIC-LoRA method is applied on top of Linear Probing for anomaly detection.

5.3. Settings

5.3.1. model hyper-parameters

The hyperparameters used for training our models are shown in the Table 4:

Table 4: Main experiment parameter settings of the TRACE method

Model	Hyper-parameters	Value
MOMENT(TRACE)	dimension of model	768
	number of layers	12
	number of heads	12
	Sequence length	512
	patch length	8
	dimension of feedforward layer	3072
	lora rank γ	2
	max rank of AdaLoRA	4
	total mask percentage	95%
	mask percentage by step	10%
	random masking operation times M	8
	forecast horizon	{192,336,720}
	Dimensionality Reduction Factor β	8

5.3.2. training hyper-parameters

For the long-term forecasting task, during the model training phase, we use a backtracking window of length $L = 512$ for training all models. We

predict the Exchange dataset with $T = 96$ and $T = 192$ time steps, while for the other datasets, the prediction horizons are set to $T = 192$ and $T = 720$ time steps. We evaluate the models using Mean Squared Error (MSE) and Mean Absolute Error (MAE) as metrics.

The initial learning rate during training is set to 2×10^{-4} , with a maximum of 15 epochs for training. The validation and test sets are split according to the rules outlined in Table 3, and we adopt the OneCycleLR strategy for early stopping. The batch size used during model training is 16.

For the short-term forecasting task, we follow the settings defined in MOMENT. For the Monthly dataset, the prediction horizon $T = 18$; for the Quarterly dataset, $T = 8$; and for the Yearly dataset, $T = 6$.

For the anomaly detection task, the training parameters remain consistent with those used in the forecasting tasks.

5.4. Main Experimental Results

5.4.1. Long-horizon Forecasting

Table 5: Long-term forecasting performance measured using Mean Squared Error (MSE) and Mean Absolute Error (MAE). Results are averaged over five random experiments. Bold and underlined values indicate the best and second-best results, respectively.

Forecasting Horizon	MOMENT _{LP}		MOMENT _{LP+LoRA}		MOMENT _{Proj down}		MOMENT _{AdaLoRA}		TRACE		
	MSE	MAE	MSE	MAE	MSE	MAE	MSE	MAE	MSE	MAE	
ETTh1	192	0.417	0.430	0.420	0.433	0.415	0.430	<u>0.414</u>	<u>0.429</u>	0.412	0.427
	336	0.432	0.449	0.435	0.450	<u>0.429</u>	<u>0.446</u>	0.430	<u>0.446</u>	0.428	0.444
	720	0.476	0.487	0.479	0.490	0.475	0.486	<u>0.472</u>	<u>0.484</u>	0.470	0.481
ETTh2	192	0.347	0.389	0.348	0.388	0.347	0.386	0.345	0.384	0.346	0.385
	336	0.374	0.413	0.376	0.417	<u>0.373</u>	<u>0.412</u>	0.376	0.416	0.370	0.409
	720	0.397	0.436	0.398	0.437	<u>0.396</u>	<u>0.435</u>	0.399	0.437	0.395	0.434
ETTm1	192	0.328	0.368	0.329	0.371	<u>0.327</u>	<u>0.367</u>	0.330	0.372	0.326	0.366
	336	0.355	0.388	0.356	0.389	0.353	0.387	<u>0.352</u>	<u>0.386</u>	0.351	0.384
	720	0.408	0.419	0.411	0.422	<u>0.406</u>	<u>0.417</u>	0.407	0.418	0.405	0.416
ETTm2	192	0.228	0.299	0.229	0.300	0.226	0.297	0.227	0.298	0.228	0.299
	336	0.276	0.329	0.279	0.331	0.276	0.328	0.275	0.327	0.274	0.325
	720	0.360	0.386	0.362	0.387	<u>0.360</u>	<u>0.384</u>	0.363	0.388	0.359	0.383
Weather	192	0.204	0.254	0.207	0.258	<u>0.203</u>	<u>0.252</u>	0.206	0.257	0.200	0.248
	336	0.253	0.294	0.255	0.296	<u>0.252</u>	<u>0.293</u>	0.254	0.296	0.251	0.292
	720	0.323	0.340	0.324	0.340	0.321	0.339	<u>0.318</u>	<u>0.338</u>	0.317	0.337
Exchange	96	0.122	0.249	0.119	0.247	0.105	0.230	0.111	0.237	<u>0.108</u>	<u>0.233</u>
	192	0.225	0.342	0.222	0.340	0.214	0.333	<u>0.210</u>	<u>0.329</u>	0.206	0.326
	336	0.317	0.434	0.320	0.437	<u>0.315</u>	<u>0.433</u>	0.316	0.434	0.313	0.430
ECL	192	0.158	0.254	0.160	0.255	0.153	0.248	0.149	0.244	<u>0.151</u>	0.246
	336	<u>0.169</u>	<u>0.266</u>	0.172	0.268	0.170	0.267	0.171	0.267	0.167	0.264
	720	0.210	0.301	<u>0.209</u>	<u>0.300</u>	0.208	0.298	0.210	0.301	0.208	0.298

Table 5 presents the main experimental results for long-term forecasting, comparing the performance of the MOMENT model under five conditions: linear probing, full LoRA fine-tuning, reconstruction of the forecasting head (projection down, with $\beta = 8$), AdaLoRA (with projection down head) and TRACE (Gated DSIC and projection down with $\beta = 8$) fine-tuning. The results are evaluated in terms of MSE and MAE across different prediction lengths.

By comparing the results, we observe that the reconstructed forecasting head: $\text{MOMENT}_{Proj\ down}$, achieves lower MSE and MAE across all long-term forecasting tasks compared to linear probing (MOMENT_{LP}) and full LoRA fine-tuning ($\text{MOMENT}_{LP+LoRA}$). Our proposed **TRACE** outperforms other approaches, including AdaLoRA, on the majority of datasets.

Static Test: We further conducted a statistical significance test (McNemar’s test, p -value=0.0071) on the prediction errors, which confirms that TRACE’s improvements over MOMENT_{LP} are statistically significant.

The detailed methodology and results of this test are provided in Appendix Appendix B

Computational Cost: To address concerns regarding the computational overhead of our Gated DSIC importance evaluation, we provide a detailed breakdown of training and inference costs on the Electricity dataset (prediction horizon = 720, $\beta = 4$) in Table 6. Our TRACE method requires 942.86 seconds of training time, which is approximately $1.30\times$ that of full LoRA (729.58s) and $1.47\times$ that of AdaLoRA (643.31s). This modest increase in training time is solely attributed to the offline Monte Carlo importance evaluation on the validation set and is deemed acceptable given the consistent performance gains demonstrated in Table 5. Crucially, the inference time of the final pruned TRACE model (38.17s) is nearly identical to that of AdaLoRA (37.95s) and full LoRA (38.36s), confirming that our method imposes no additional latency during deployment. Furthermore, TRACE achieves the lowest backbone parameter count (2.89M) among all PEFT baselines, enhancing its efficiency for resource-constrained scenarios. In summary, the slight offline training overhead is a worthwhile trade-off for a more effective and deployment-ready fine-tuned model.

Table 6: Computational cost on Electricity dataset.

	Models	Parameters(M)	Trainging time(s)	Inference time (s)
Forecasting Head	linear probing	35.38	387.32	41.70
	Proj Down	8.99	251.34	27.45
	Avg Pool	8.99	223.56	26.34
	Less Feature	8.47	219.95	27.12
	Conv2D	8.84	260.17	33.43
Backbone	full LoRA	4.75	729.58	38.36
	AdaLoRA	3.43	643.31	37.95
	TRACE	2.89	942.86	38.17

5.4.2. Short-horizon Forecasting

Table 7: Zero-shot short-horizon forecasting performance on a subset of the M3 and M4 datasets measured using sMAPE.

Datasets	MOMENT _{LP}		MOMENT _{LP+LoRA}		MOMENT _{Proj down}		TRACE	
	M4	FR	M4	FR	M4	FR	M4	FR
M3	Yearly	17.03	17.13	17.21	17.37	17.01	17.85	16.88 17.49
	Quarterly	10.47	10.73	10.81	11.36	10.34	10.74	10.25 10.70
	Monthly	16.35	17.11	16.49	17.26	16.32	17.10	16.28 17.03
M4	Yearly	-	15.11	-	15.37	-	14.98	- 14.83
	Quarterly	-	12.86	-	13.14	-	12.55	- 12.03
	Monthly	-	16.26	-	16.73	-	15.98	- 15.87

For short-horizon forecasting, we adopt the zero-shot setting proposed by Oreshkin [28]. Specifically, we first fine-tune MOMENT on a **source dataset** with a forecasting head and then assess its performance on a **target dataset** without any additional fine-tuning. It is consistent with the setup in MOMENT [1].

We evaluated our model’s zero-forecasting performance on the M3 and M4 datasets. We maintained the same settings as in the MOMENT[1], following the dataset splits for training, testing, and forecasting horizons as defined in the M3 and M4 competitions. The evaluation metric used was sMAPE ([29]; [30]). Due to the scarcity of daily, hourly, and weekly frequency data, it is challenging for deep models to fully leverage their zero-shot capabilities in these cases. Table 8 presents the correspondence between source and target datasets. The setup for the Fred dataset follows [1] and [28].

Table 7 show that, under the sMAPE evaluation metric, the reconstructed forecasting head (MOMENT_{Proj down}) and the TRACE method both outper-

Table 8: Experimental settings for short-horizon forecasting experiments for varying source and target datasets.

Source Dataset → Target ↓	M4	Fred
M4		
Yearly	-	Yearly
Quarterly	-	Yearly
Monthly	-	Monthly
M3		
Yearly	Yearly	Yearly
Quarterly	Quarterly	Quarterly
Monthly	Monthly	Monthly

form linear probing and full fine-tuning.

5.4.3. Anomaly Detection

Table 9: Anomaly detection performance on selected datasets from the UCR Anomaly Archive

Adj-F1	MITDB	ECG			MGAB			SVDB	
Index	100	801	803	1406	2	3	4	842	859
MOMENT _{LP}	0.819	0.695	0.968	0.761	0.429	0.437	0.459	0.828	0.864
TRACE	0.820	0.702	0.969	0.761	0.444	0.448	0.460	0.828	0.865

In the anomaly detection task, we selected subsets of datasets from MITDB, ECG, MGAB, and SVDB. Since the task of anomaly detection involves a relatively small number of parameters in the forecasting head, which is not suitable for dimensionality reduction or reconstruction, in this context, TRACE is equivalent to Gated DSIC. Table 9 show that TRACE generally outperforms the linear probing.

5.4.4. Natural Language Processing Task

While our work focuses on continuous temporal data, evaluating on natural language tasks is necessary to assess the method’s applicability across sequential modalities. As natural language represents discrete sequences, such comparison reveals the adaptability and robustness of our approach beyond traditional time series, offering valuable insights into its generalization across both low- and high-frequency domains. These findings can serve as a reference and inspiration for future research exploring the intersection of temporal modeling and discrete sequence processing.

Table 10: Overall comparison on the GLUE benchmark with the DeBERTaV3-base backbone. Results are averaged over five random experiments. Bold and underlined values indicate the best and second-best results, respectively. The initial LoRA rank is set to 4 and then halved according to our method.

Method	Trainable Params	Avg. Score	MNLI	QQP	QNLI	SST-2	CoLA	STS-B	MRPC	RTE
Full Fine-tuning	184M	88.62	90.01	91.10	94.03	95.63	69.19	91.60	89.46	86.94
Adapter	0.35M	87.57	90.28	89.41	93.52	94.38	67.80	91.08	89.75	84.36
LoRA	0.33M	88.12	90.34	90.26	93.87	94.84	68.71	91.63	89.71	85.56
AdaLoRA	0.35M	88.93	90.18	90.37	<u>94.29</u>	95.62	70.04	91.57	<u>90.34</u>	87.06
MOELoRA	0.92M	88.89	90.26	90.31	94.08	95.53	70.47	91.52	90.26	<u>87.64</u>
DoRA	0.33M	<u>89.00</u>	<u>90.43</u>	90.16	94.17	<u>95.80</u>	70.26	<u>91.68</u>	90.12	87.38
Proposed Method										
Our Method	0.33M	89.51	90.76	<u>90.66</u>	94.72	96.17	<u>71.95</u>	92.33	90.86	88.63

Table 11: Comparison of different PEFT methods for two backbone models (Qwen2.5 0.5B). Results are presented as accuracy for each task and averaged across five random experiments. The LLM used is the Qwen2.5 0.5B model, with the LoRA rank initially set to 32 and then halved.

Method (Million)	Trainable Params (acc)	BoolQ (acc)	ARC-e (acc)	ARC-c (acc)
Baseline(Qwen2.5 0.5B)				
Adapter	9.0M	78.36	71.04	53.26
LoRA	8.8M	78.94	72.78	54.38
AdaLoRA	8.9M	80.32	73.96	54.23
Our Method	8.8M	82.49	74.67	55.64

We are currently conducting experiments on English datasets in the field of natural language processing. The datasets are sourced from the GLUE benchmark: paraphrase detection (MRPC, QQP), sentiment classification (SST-2), natural language inference (MNLI, RTE, QNLI), and linguistic acceptability (CoLA). We also consider three challenging QA datasets to evaluate the performance of our method on large language models: three common-sense question-answering benchmark tasks—ARC-e, ARC-c [31], and BoolQ [32].

Experimental results on the GLUE benchmark are shown in Table 10, and those on the QA datasets are presented in Table 11. Our method, Gated-DSIC, achieves the best or second-best performance with the smallest number of trainable parameters in both settings.

5.5. Ablation studies and further analysis

In this section, we analyze the effects of dimensionality reduction factor β , forecasting head reconstruction methods, and LoRA rank on model performance. Results indicate that excessively large β degrades accuracy, with optimal values typically being 4 or 8. For long-horizon forecasting, reconstruction method performance varies by task. Additionally, LoRA rank should remain moderate to avoid overfitting, as the pre-trained time-series backbone requires only minimal fine-tuning on the target dataset. Ablation studies confirm TRACE's strong stability.

5.5.1. Impact of the Dimensionality Reduction Factor β

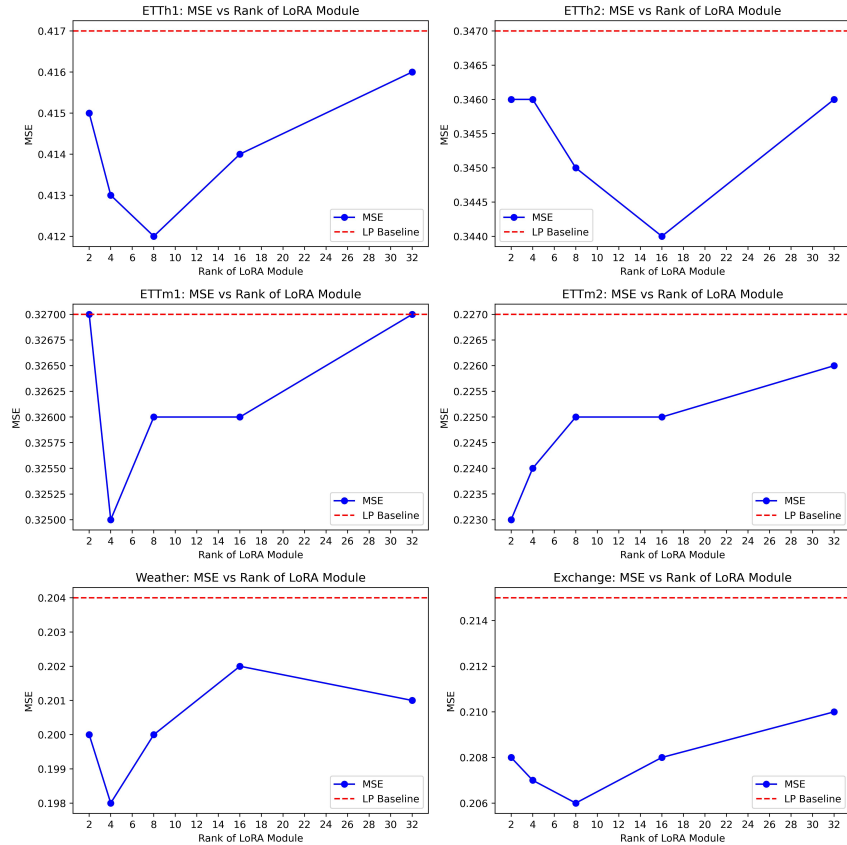


Figure 6: MSE Comparison between TRACE Method and Linear Probing on Different Datasets at Different β (Prediction Horizon: 192, Forecasting Head: Projection Down)

Figure 6 illustrates the effect of varying the dimensionality reduction factor on MSE under the TRACE method, with a forecast horizon of 192 and the Projection Down reconstruction for different tasks. The analysis shows that the overall fluctuation is minimal, with the maximum fluctuation in a single task not exceeding 1%. The optimal dimensionality reduction factor, β , typically takes values of 4 or 8. A larger value of β reduces the number of trainable parameters in the forecasting head, which in turn negatively impacts the model's forecasting performance. Figure 7 presents the results for a forecast horizon of 720, where similar conclusions can be drawn.

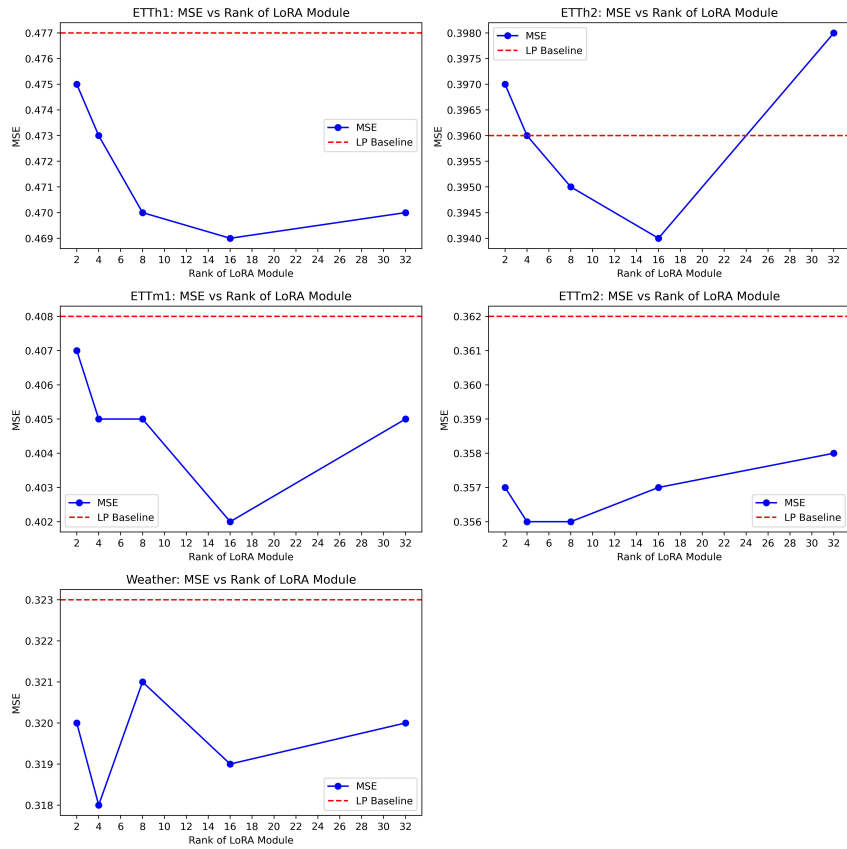


Figure 7: MSE Comparison between TRACE Method and Linear Probing on Different Datasets at Different β (Prediction Horizon: 720, Forecasting Head: Projection Down)

5.5.2. Impact of Different Forecasting Heads

Table 12: Long-term forecasting performance measured using Mean Squared Error (MSE) and Mean Absolute Error (MAE) in different reconstruction forecasting head. Bold values indicate the best.

Forecasting Horizon	MOMENT _{LP}		TRACE _{Less Feature}		TRACE _{Avg Pool}		TRACE _{Conv2D}		TRACE _{Proj Down}		
	MSE	MAE	MSE	MAE	MSE	MAE	MSE	MAE	MSE	MAE	
ETTh1	192	0.417	0.430	0.413	0.428	0.414	0.429	0.423	0.435	0.412 0.427	
	336	0.432	0.449	0.428	0.445	0.427	0.443	0.437	0.455	0.428	0.444
	720	0.476	0.487	0.469	0.480	0.471	0.482	0.479	0.491	0.470	0.481
ETTh2	192	0.347	0.389	0.347	0.388	0.345	0.386	0.353	0.394	0.345 0.385	
	336	0.374	0.413	0.369	0.407	0.368	0.407	0.377	0.417	0.370	0.409
	720	0.396	0.435	0.395	0.434	0.396	0.435	0.416	0.457	0.395 0.434	
ETTm1	192	0.327	0.368	0.326	0.367	0.325	0.365	0.333	0.375	0.326	0.366
	336	0.355	0.388	0.351	0.385	0.352	0.386	0.354	0.388	0.351 0.384	
	720	0.408	0.419	0.403	0.414	0.404	0.415	0.417	0.428	0.405	0.416
ETTm2	192	0.227	0.299	0.228	0.300	0.226	0.298	0.231	0.305	0.228	0.299
	336	0.276	0.329	0.276	0.328	0.273	0.325	0.287	0.339	0.274	0.325
	720	0.360	0.386	0.358	0.384	0.354	0.380	0.373	0.401	0.359	0.383
Weather	192	0.204	0.254	0.201	0.248	0.200	0.248	0.211	0.260	0.200 0.248	
	336	0.253	0.294	0.250	0.291	0.251	0.293	0.267	0.308	0.251	0.292
	720	0.323	0.340	0.319	0.339	0.317	0.336	0.328	0.345	0.317	0.337
Exchange	96	0.122	0.249	0.103	0.228	0.105	0.229	0.119	0.245	0.108	0.233
	192	0.225	0.342	0.211	0.330	0.208	0.327	0.228	0.345	0.206 0.326	
	336	0.317	0.434	0.314	0.432	0.312	0.430	0.329	0.347	0.313	0.430

Under the condition of the same dimensionality reduction factor ($\beta = 8$), we compared the performance of the TRACE method with different reconstruction approaches for the forecasting head and the original linear probing method on long-term forecasting datasets. Specifically, TRACE_{Proj Down}, TRACE_{Less Feature}, TRACE_{Avg Pool}, and TRACE_{Conv2D} refer to the different forecasting head reconstruction methods previously introduced.

The comparison results in Table 12, in nearly all tasks, the TRACE method outperforms Linear Probing or performs equivalently. However, when reconstructing the forecasting head with Conv2D, the performance is generally suboptimal, and in most cases, it is inferior to Linear Probing, with a performance gap of within 3.8%. A possible reason for this is that 2D convolution may not be well-suited for extracting features from time series with independent channels, as fluctuations between covariates can introduce interference.

However, the performance of different reconstruction methods varies across tasks, with no single method being consistently optimal for all tasks. This suggests that, in practical applications, it may be beneficial to tailor the

forecasting head to suit the specific task at hand.

5.5.3. Impact of LoRA Rank

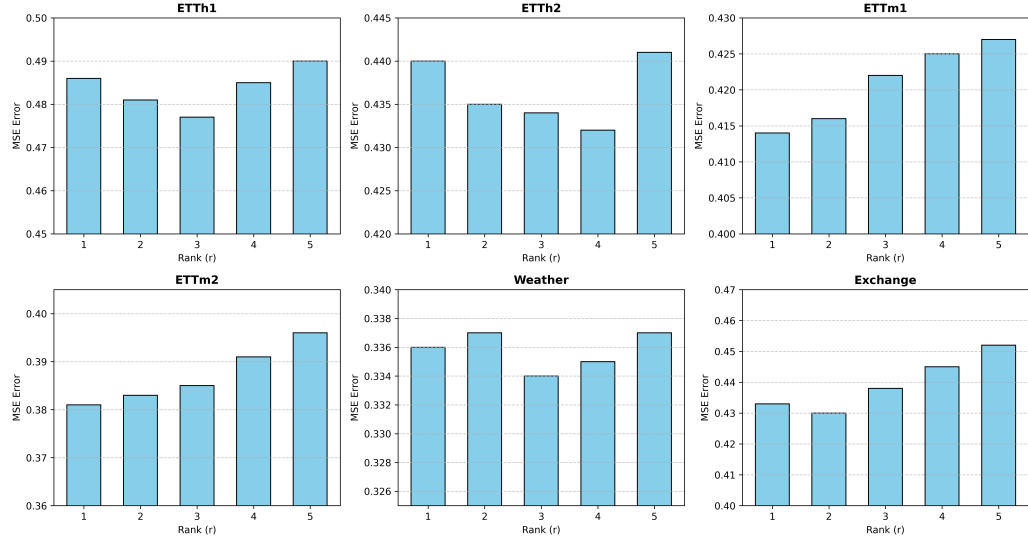


Figure 8: The impact of the rank size of the incremental matrix on model performance measured using Mean Squared Error (MSE)

Figure 8 illustrates the performance variations of the TRACE method on different long-term forecasting datasets when only the LoRA rank γ is changed, while keeping all other parameters consistent with the main experiment settings. The analysis indicates that the optimal rank value falls within the range of 2 to 3. This ablation study also confirms that when fine-tuning time series foundation models with LoRA, selecting an excessively large rank γ is not advisable.

5.5.4. Case Analysis

We conducted a case analysis on four ETT datasets (ETTh1, ETTh2, ETTm1, and ETTm2) by plotting the ground truth time series of the test set along with the predicted sequences from MOMENT_{LP} , $\text{MOMENT}_{Proj\ down}$, and $\text{TRACE}_{Proj\ Down}$, as illustrated in Figure 9. In the figure, the predictions generated by the TRACE method are represented by the yellow curve, which more closely aligns with the green curve denoting the ground truth compared to the results from other models.

To provide a more intuitive comparison, we visualize partial forecasts on the ETTh2 test set. For a prediction horizon of 192 (Figure 10, TRACE in Figure 10f), our method shows better alignment with the true values, especially during volatile periods (e.g., steps 460–500). With a horizon of 720 (Figure 11), TRACE in Figure 11f captures the drop trend around step 500 more accurately than competing methods.

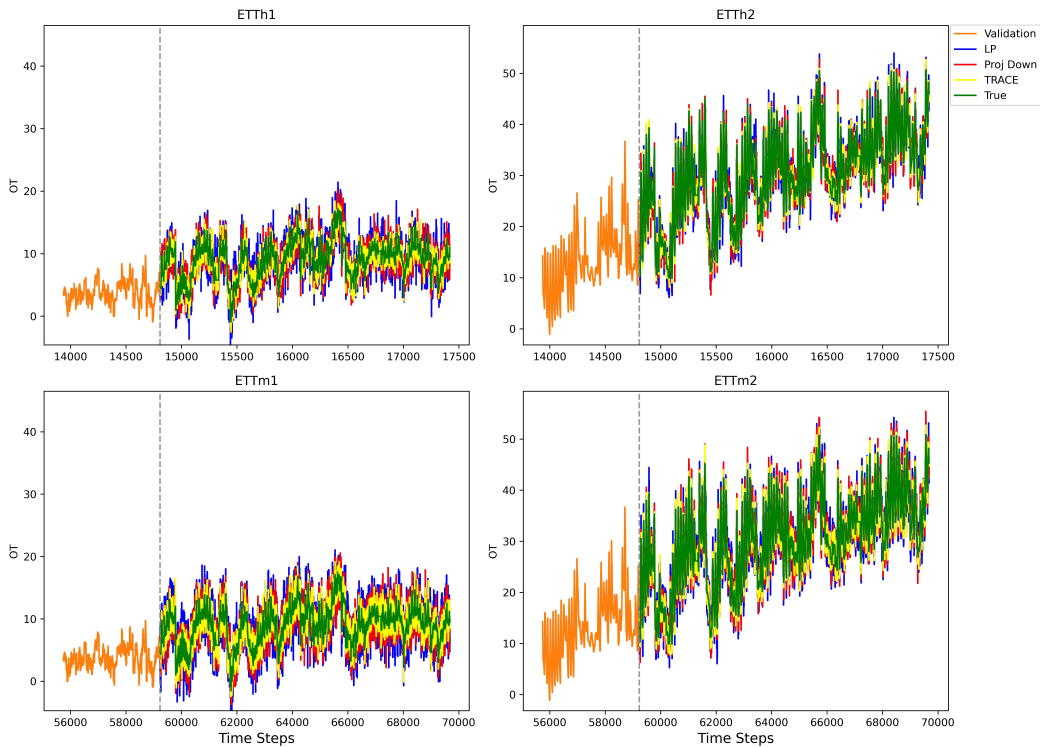


Figure 9: Comparison of true values on the ETT long-horizon forecasting dataset’s test set with predicted values from different models

5.6. Conclusions and future work

In this work, we presented TRACE, a parameter-efficient fine-tuning framework tailored for time series foundation models. Our approach addresses two critical bottlenecks: the parameter inefficiency of standard forecasting heads and the biased importance evaluation in existing PEFT methods. Through extensive experiments, we demonstrated that TRACE’s recon-

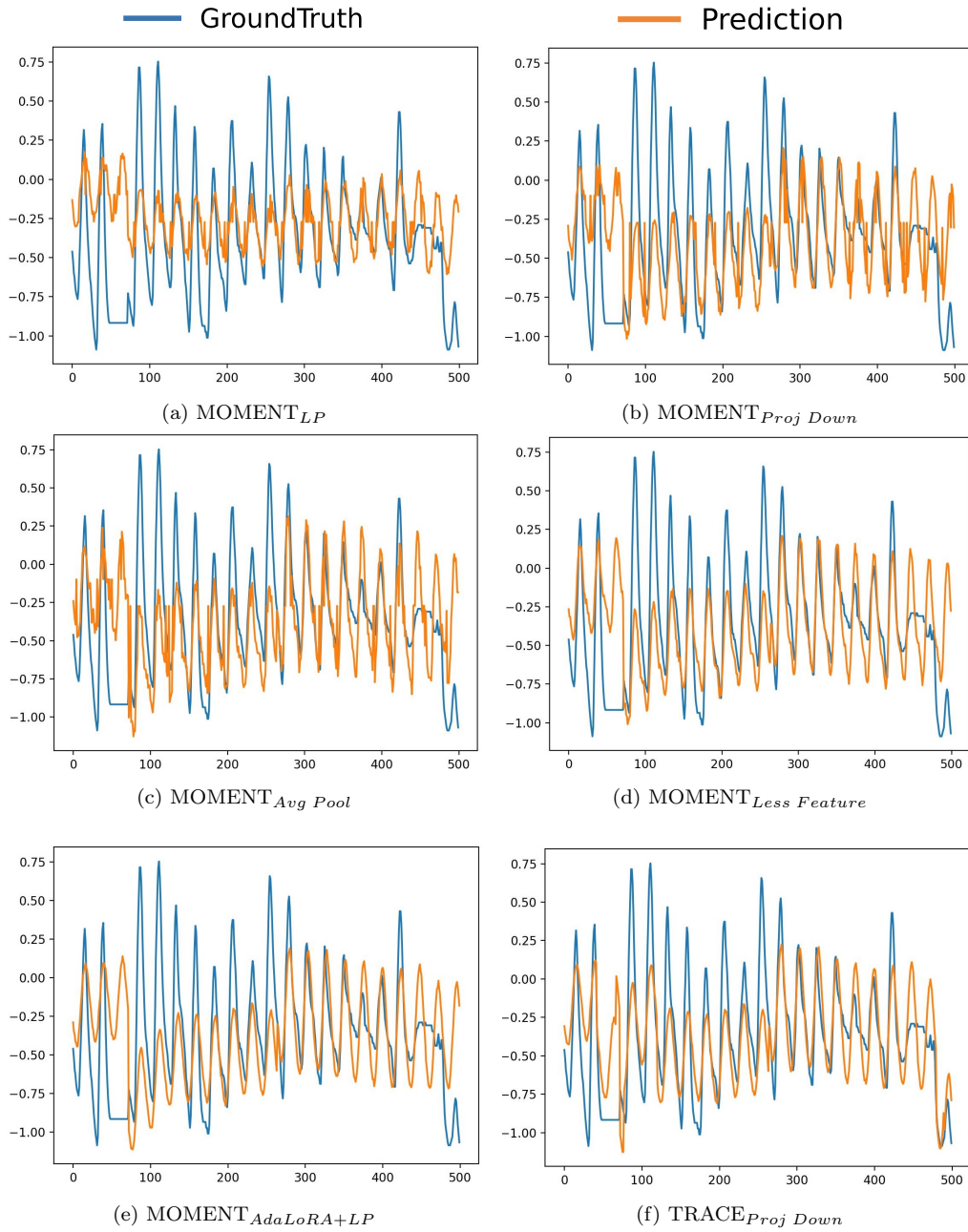


Figure 10: Forecasting cases using the input-512-predict-192 configuration.

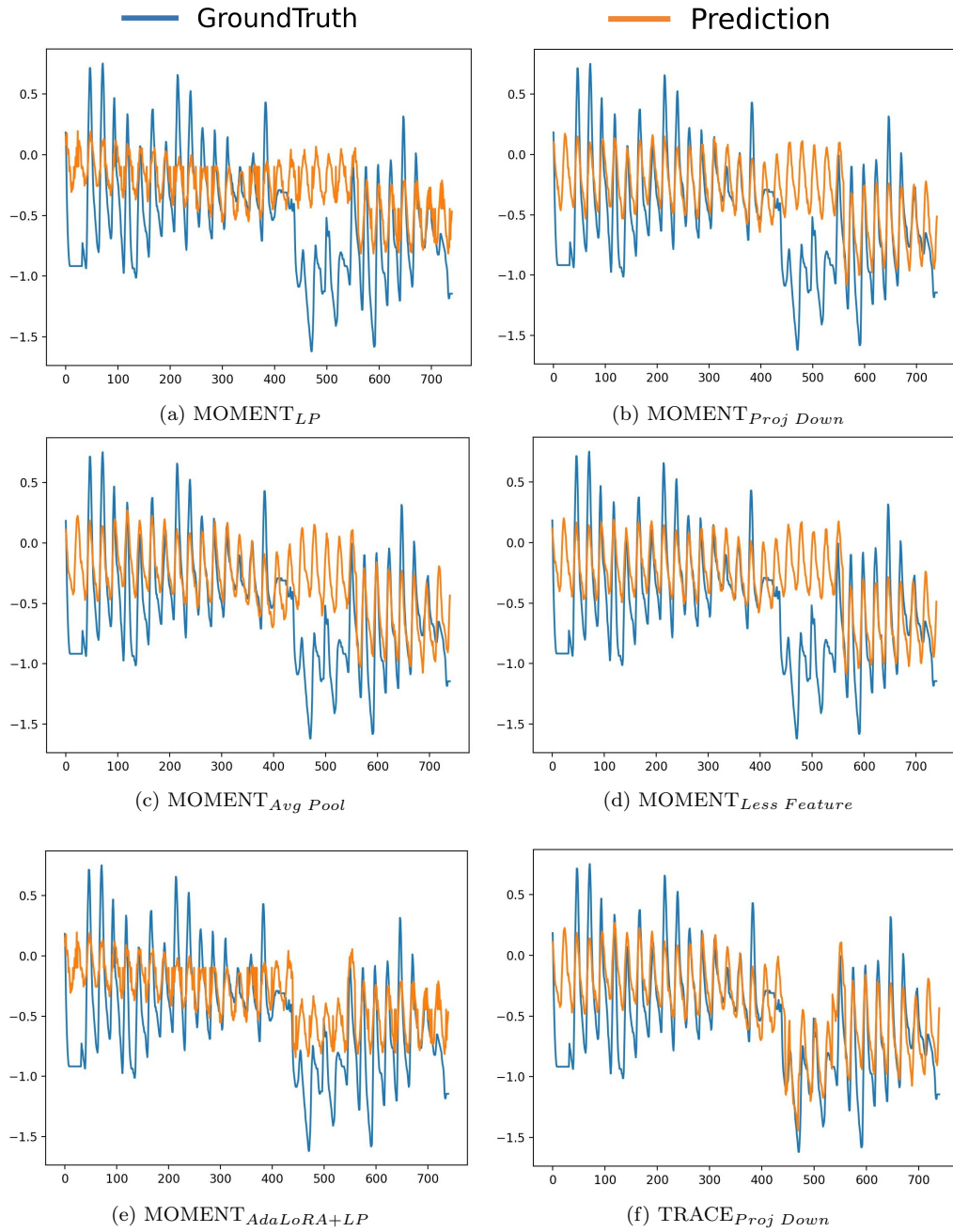


Figure 11: Forecasting cases using the input-512-predict-720 configuration.

structured heads and the Gated DSIC mechanism consistently yield superior performance across a range of tasks.

A current limitation is that the optimal set of LoRA modules may vary across tasks. For future work, we plan to investigate task-agnostic or meta-learning-based strategies to identify a universal set of adaptable modules. Furthermore, we aim to explore the integration of TRACE with multimodal time series (e.g., combining sensor data with textual logs) to unlock new applications in real-world scenarios.

References

- [1] M. Goswami, K. Szafer, A. Choudhry, Y. Cai, S. Li, A. Dubrawski, Moment: A family of open time-series foundation models, arXiv preprint arXiv:2402.03885 (2024).
- [2] R. J. Hyndman, A. B. Koehler, R. D. Snyder, S. Grose, A state space framework for automatic forecasting using exponential smoothing methods, International Journal of forecasting 18 (3) (2002) 439–454.
- [3] A. A. Ariyo, A. O. Adewumi, C. K. Ayo, Stock price prediction using the arima model, in: 2014 UKSim-AMSS 16th international conference on computer modelling and simulation, IEEE, 2014, pp. 106–112.
- [4] J. H. Stock, M. W. Watson, Vector autoregressions, Journal of Economic perspectives 15 (4) (2001) 101–115.
- [5] T. Chen, C. Guestrin, Xgboost: A scalable tree boosting system, in: Proceedings of the 22nd ACM SIGKDD international conference on knowledge discovery and data mining, 2016, pp. 785–794.
- [6] G. Ke, Q. Meng, T. Finley, T. Wang, W. Chen, W. Ma, Q. Ye, T.-Y. Liu, Lightgbm: A highly efficient gradient boosting decision tree, Advances in neural information processing systems 30 (2017).
- [7] S. Hochreiter, J. Schmidhuber, Long short-term memory, Neural computation 9 (8) (1997) 1735–1780.
- [8] J. Chung, C. Gulcehre, K. Cho, Y. Bengio, Empirical evaluation of gated recurrent neural networks on sequence modeling, arXiv preprint arXiv:1412.3555 (2014).
- [9] C. Lea, M. D. Flynn, R. Vidal, A. Reiter, G. D. Hager, Temporal convolutional networks for action segmentation and detection, in: proceedings of the IEEE Conference on Computer Vision and Pattern Recognition, 2017, pp. 156–165.
- [10] A. Vaswani, N. Shazeer, N. Parmar, J. Uszkoreit, L. Jones, A. N. Gomez, Ł. Kaiser, I. Polosukhin, Attention is all you need, Advances in neural information processing systems 30 (2017).

- [11] H. Zhou, S. Zhang, J. Peng, S. Zhang, J. Li, H. Xiong, W. Zhang, Informer: Beyond efficient transformer for long sequence time-series forecasting, in: Proceedings of the AAAI conference on artificial intelligence, Vol. 35, 2021, pp. 11106–11115.
- [12] Y. Liu, T. Hu, H. Zhang, H. Wu, S. Wang, L. Ma, M. Long, itransformer: Inverted transformers are effective for time series forecasting, arXiv preprint arXiv:2310.06625 (2023).
- [13] T. Zhou, Z. Ma, Q. Wen, X. Wang, L. Sun, R. Jin, Fedformer: Frequency enhanced decomposed transformer for long-term series forecasting, in: International conference on machine learning, PMLR, 2022, pp. 27268–27286.
- [14] Y. Nie, N. H. Nguyen, P. Sinthong, J. Kalagnanam, A time series is worth 64 words: Long-term forecasting with transformers, arXiv preprint arXiv:2211.14730 (2022).
- [15] A. Garza, C. Challu, M. Mergenthaler-Canseco, Timegpt-1, arXiv preprint arXiv:2310.03589 (2023).
- [16] D. Cao, F. Jia, S. O. Arik, T. Pfister, Y. Zheng, W. Ye, Y. Liu, Tempo: Prompt-based generative pre-trained transformer for time series forecasting, arXiv preprint arXiv:2310.04948 (2023).
- [17] A. Das, W. Kong, R. Sen, Y. Zhou, A decoder-only foundation model for time-series forecasting, in: Forty-first International Conference on Machine Learning, 2024.
- [18] G. Woo, C. Liu, A. Kumar, C. Xiong, S. Savarese, D. Sahoo, Unified training of universal time series forecasting transformers (2024).
- [19] S. Gao, T. Koker, O. Queen, T. Hartvigsen, T. Tsilgkaridis, M. Zitnik, Units: Building a unified time series model, arXiv e-prints (2024) arXiv–2403.
- [20] C. Sun, H. Li, Y. Li, S. Hong, Test: Text prototype aligned embedding to activate llm’s ability for time series, arXiv preprint arXiv:2308.08241 (2023).

- [21] M. Jin, S. Wang, L. Ma, Z. Chu, J. Y. Zhang, X. Shi, P.-Y. Chen, Y. Liang, Y.-F. Li, S. Pan, et al., Time-llm: Time series forecasting by reprogramming large language models, arXiv preprint arXiv:2310.01728 (2023).
- [22] K. Rasul, A. Ashok, A. R. Williams, A. Khorasani, G. Adamopoulos, R. Bhagwatkar, M. Biloš, H. Ghonia, N. Hassen, A. Schneider, et al., Lag-llama: Towards foundation models for time series forecasting, in: R0-FoMo: Robustness of Few-shot and Zero-shot Learning in Large Foundation Models, 2023.
- [23] N. Shazeer, Glu variants improve transformer, arXiv preprint arXiv:2002.05202 (2020).
- [24] W. Held, D. Yang, Shapley head pruning: Identifying and removing interference in multilingual transformers, arXiv preprint arXiv:2210.05709 (2022).
- [25] H. Zhou, S. Zhang, J. Peng, S. Zhang, J. Li, H. Xiong, W. Zhang, Informer: Beyond efficient transformer for long sequence time-series forecasting, in: The Thirty-Fifth AAAI Conference on Artificial Intelligence, AAAI 2021, Virtual Conference, Vol. 35, AAAI Press, 2021, pp. 11106–11115.
- [26] R. Godahewa, C. Bergmeir, G. I. Webb, R. J. Hyndman, P. Montero-Manso, Monash time series forecasting archive, arXiv preprint arXiv:2105.06643 (2021).
- [27] J. Paparrizos, Y. Kang, P. Boniol, R. S. Tsay, T. Palpanas, M. J. Franklin, Tsb-uad: an end-to-end benchmark suite for univariate time-series anomaly detection, Proceedings of the VLDB Endowment 15 (8) (2022) 1697–1711.
- [28] B. N. Oreshkin, D. Carpov, N. Chapados, Y. Bengio, Meta-learning framework with applications to zero-shot time-series forecasting, in: Proceedings of the AAAI conference on artificial intelligence, Vol. 35, 2021, pp. 9242–9250.
- [29] B. N. Oreshkin, D. Carpov, N. Chapados, Y. Bengio, N-beats: Neural basis expansion analysis for interpretable time series forecasting, arXiv preprint arXiv:1905.10437 (2019).

- [30] H. Wu, T. Hu, Y. Liu, H. Zhou, J. Wang, M. Long, Timesnet: Temporal 2d-variation modeling for general time series analysis, arXiv preprint arXiv:2210.02186 (2022).
- [31] P. Clark, I. Cowhey, O. Etzioni, T. Khot, A. Sabharwal, C. Schoenick, O. Tafjord, Think you have solved question answering? try arc, the ai2 reasoning challenge, arXiv preprint arXiv:1803.05457 (2018).
- [32] C. Clark, K. Lee, M.-W. Chang, T. Kwiatkowski, M. Collins, K. Toutanova, Boolq: Exploring the surprising difficulty of natural yes/no questions, arXiv preprint arXiv:1905.10044 (2019).
- [33] H. Jiang, D. Liu, X. Ding, Y. Chen, H. Li, Tcm: An efficient lightweight mlp-based network with affine transformation for long-term time series forecasting, Neurocomputing 617 (2025) 128960.

Appendix A. Multiple Variants of Reconstructed Forecasting Heads and Their Parameter Complexity

Proj Down: A factorized linear architecture reduces dimensions via two projections. For input $\mathbf{X} \in \mathbb{R}^{B \times N \times D}$ (B : batch size, N : patches, D : embedding dimension), a learnable projection $\mathbf{W}_1 \in \mathbb{R}^{D \times D/\beta}$ reduces D by factor β , yielding $\mathbf{X}' = \mathbf{X}\mathbf{W}_1$. Flattened features $\text{Flatten}(\mathbf{X}') \in \mathbb{R}^{B \times (N \cdot D/\beta)}$ are projected via $\mathbf{W}_2 \in \mathbb{R}^{(N \cdot D/\beta) \times H}$ to produce horizon predictions $\hat{\mathbf{Y}} \in \mathbb{R}^{B \times H}$. This reduces parameters from $\mathcal{O}(NDH)$ to $\mathcal{O}(D^2/\beta + NDH/\beta)$.

Less Feature: Non-learnable truncation retains only the first D/β dimensions along the feature axis: $\mathbf{X}' = \mathbf{X}_{\dots, :D/\beta}$. Flattened features $\text{Flatten}(\mathbf{X}') \in \mathbb{R}^{B \times (N \cdot D/\beta)}$ are mapped to horizon H via $\mathbf{W} \in \mathbb{R}^{(N \cdot D/\beta) \times H}$. Parameter complexity is $\mathcal{O}(NDH/\beta)$, trading simplicity for potential information loss.

Avg Pool: Spatial pooling combines 2D average pooling and learnable projection. Input $\mathbf{X} \in \mathbb{R}^{B \times C \times N \times D}$ (C : channels) is spatially downsampled via AvgPool2d:

$$\mathbf{X}' = \text{AvgPool2d}(\mathbf{X}), \quad \mathbf{X}' \in \mathbb{R}^{B \times C \times N/2 \times D}. \quad (\text{A.1})$$

A linear layer $\mathbf{W}_1 \in \mathbb{R}^{D \times D/\beta}$ compresses features, and flattened features $\text{Flatten}(\mathbf{X}'') \in \mathbb{R}^{B \times (C \cdot N/2 \cdot D/\beta)}$ are mapped to horizon H via \mathbf{W}_2 . This balances locality preservation and efficiency.

Conv 2D: Temporal convolution employs strided depthwise 1D convolutions for subsampling. For input $\mathbf{X} \in \mathbb{R}^{B \times C \times N \times D}$, a kernel $\mathbf{K} \in \mathbb{R}^{1 \times k}$ with stride $s = \beta$ operates along the temporal axis:

$$\mathbf{X}' = \text{Conv2d}(\mathbf{X}), \quad \mathbf{X}' \in \mathbb{R}^{B \times C \times \lfloor N/s \rfloor \times D}. \quad (\text{A.2})$$

Convolution reduces sequence length by β , followed by a linear layer $\mathbf{W} \in \mathbb{R}^{(C \cdot \lfloor N/s \rfloor \cdot D) \times H}$. Parameter cost is $\mathcal{O}(k)$ for convolution and $\mathcal{O}(NDH/\beta)$ for projection.

Appendix B. Statistical Validation of Performance

To evaluate the performance of our proposed TRACE model against the state-of-the-art MOMENT_{LP} , we conducted a statistical analysis using the dataset’s actual values and the predictions from both models. Our objective was to assess the accuracy and reliability of these models under various conditions.

To quantify predictive performance, we employed a binary classification framework. A prediction was considered accurate if the absolute error between the predicted and actual values was below a predetermined threshold of 5.0[33]; otherwise, it was deemed inaccurate.

We constructed a 2×2 contingency table to systematically categorize the predictive outcomes of both models. The confusion matrix for the classification results is as follows:

$$\begin{bmatrix} 158993571 & 1108 \\ 985 & 4932 \end{bmatrix}.$$

The four categories were defined as: both models correctly predicted (158993571 instances), TRACE correctly predicted while MOMENT_{LP} incorrectly predicted (1108 instances), TRACE incorrectly predicted while MOMENT_{LP} correctly predicted (985 instances), and both models incorrectly predicted (4932 instances). This classification enabled a detailed comparative analysis of the models’ performance.

To statistically validate the observed differences in misclassification rates, we applied the McNemar test. This non-parametric test is particularly suitable for paired nominal data, such as the binary outcomes observed in this study. The McNemar test statistic is computed as: $\chi^2 = \frac{(b-c)^2}{b+c}$, where b represents the number of cases where TRACE incorrectly predicted while

MOMENT_{LP} correctly predicted, and c represents the number of cases where TRACE correctly predicted while MOMENT_{LP} incorrectly predicted.

The test results yielded a McNemar statistic of 7.23 with an associated p-value of 0.0071. Given the conventional alpha level of 0.05, the p-value indicates a statistically significant difference in the proportion of misclassifications between the two models. Specifically, the results suggest that TRACE consistently produced more correct predictions in cases where MOMENT_{LP} failed, indicating that TRACE may offer superior performance in certain scenarios.

Appendix C. Computational Resources

Hardware :

- GPU: NVIDIA V100 (32GB memory) \times 2
- CPU: Xeon(R) Platinum 8481C, 25 cores
- RAM: 150GB

Software :

- Operating System: Ubuntu 20.04 LTS
- Deep Learning Framework: PyTorch 1.12.1
- CUDA Version: 11.6